Stabilization of Metastable Face-Centered Cubic Cobalt and the Tetragonal Phase of Zirconia by a Carbon Shell: Reaction under Autogenic Pressure at Elevated Temperature of $CoZr_2(acac)_2(O^iPr)_8$

Swati V. Pol,[†] Vilas G. Pol,[†] Gulaim Seisenbaeva,[‡] Vadim G. Kessler,[‡] and A. Gedanken*,[†]

Department of Chemistry, Bar-Ilan University, Ramat-Gan, 52900 Israel, and Department of Chemistry, SLU, Box 7015, 75007 Uppsala, Sweden

Received February 1, 2004. Revised Manuscript Received February 26, 2004

Spherical Co and ZrO_2 particles in the size range of 11−16 nm, exhibiting at room temperature metastable phases, fcc for cobalt and tetragonal for zirconia, were synthesized, by the reaction under autogenic pressure at elevated temperature (RAPET) technique. The tetragonal phase in ZrO_2 was obtained without doping the ZrO_2 with trivalent impurities. Using high-resolution transmission electron microscopy and selected area energy-dispersive X-ray analysis it is manifested that a carbon shell of ∼4 nm thickness is formed on the surface of Co and ZrO_2 nanocrystallites. This carbon shell is responsible for stabilizing the high-temperature metastable phases at room temperature. These two products were obtained by the dissociation of $CoZr_2(acac)_2(O^iPr)_8$ at 700 °C under its autogenic pressure.

Introduction

Zirconia (ZrO_2) is a well-known ceramic material that exhibits tetragonal-to-monoclinic martenstic phase transformation. This phase transformation is of technological importance as it contributes to the toughening of the ceramics.[1] The tetragonal-to-monoclinic phase transformation is accompanied by volume expansion and can be triggered by hydrostatic and shear stresses.[2] Zirconia is used as a dispersed phase in oxide (alumina)[3] as well as non-oxide (carbides, borides, and nitrides)[4] ceramics to increase their fracture toughness, strength, and hardness. This stress-induced transformation has also been shown to increase the plasticity from the shape deformation and accommodation strains, which are associated with the transformation.[5] The tetragonal zirconia phase also has a higher ionic conductivity[6] and is used in solid oxide fuel cells (SOFC). Increase in the wear and corrosion resistance of nanostructured ceramic coatings as a result of stress-induced phase transformation has also been reported.[7] Besides this, tetragonal ZrO_2 also find application as catalyst/catalyst support for various gas-phase reactions.[8,9] Hence, synthesizing ZrO_2 particles with metastable tetragonal crystal structure is important. Doping zirconia with trivalent impurities has been a traditional approach for stabilizing the metastable tetragonal phase.[10] Particle size has also been observed to have its own effect on the stability of the metastable tetragonal phase in nanocrystalline zirconia.[11] The critical size was found to be 6 nm,[12] for the stabilization of 100% tetragonal phase. Shukla et al. demonstrated that, at room temperature, the stability of the metastable tetragonal phase within the submicron-sized ZrO_2 particles strongly depends on the aggregation[13] tendency of ZrO_2 nanocrystallites. The metastable face-centered cubic (fcc) phase of cobalt was also previously detected by Liu[14] et al. inside carbon nanotubes.

Reduction of oxides and oxidation of small metal particles in metal-supported catalysts is of interest from both practical and theoretical viewpoints.[15] Various groups have employed a range of wet-chemistry methods to synthesize Co−ZrO_2 catalyst. This included synthesis, characterization of cobalt supported on ZrO_2 catalysts, and their activity for the reduction[15,16] of NO with C_3H_6

* To whom correspondence should be addressed.
[†] Bar-Ilan University.
[‡] SLU.

(1) Porter, D. L.; Evans, A. G.; Heuer, A. H. *Acta Metall.* **1979**, *27*, 1649.
(2) Simha, N.; Truskinovsky, L. *Acta Metall. Mater.* **1994**, *42*, 3827.
(3) Kosmac, T.; Swain, M. V.; Claussen, N. *Mater. Sci. Eng.* **1984**, *71*, 57.
(4) Swain, M. V. *Mater. Forum* **1988**, *11*, 202.
(5) Muddle, B. C.; Kelly, P. M. *Mater. Forum* **1988**, *11*, 182.
(6) Hassan, A. A. E.; Menzler, N. H.; Blass, G.; Ali, M. E.; Buchkremer, H. P.; Stover, D. *J. Mater. Sci.* **2002**, *37* (*16*), 3467.
(7) Aita, C. R. In *Advances in Coatings Technologies for Corrosion and Wear Resistant Coatings*; TMS Annual Meeting, Warrendale, PA, 1995; p 235.
(8) Haruta, M.; Kobayashi, T.; Sano, H.; Yamada, N. *Chem. Lett.* **1987**, *829*, 405.
(9) Knell, A.; Barnickel, P.; Baiker, A.; Wokaun, A. *J. Catal.* **1992**, *137*, 306.
(10) Ping, L.; Chen, I.-W.; Penner-Hahn, J. E. *J. Am. Ceram. Soc.* **1994**, *77*, 118.
(11) Nitsche, R.; Rodewald, M.; Skandan, G.; Fuess, H.; Hahn, H. *Nanostruct. Mater.* **1996**, *7*, 535.
(12) Nitsche, R.; Winterer, M.; Hahn, H. *Nanostruct. Mater.* **1995**, *6*, 679.
(13) Shukla, S.; Seal S.; Vij, R.; Bandyopadhyay, Sri; Rahman, Z. *Nano Lett.* **2002**, *2*, 989.
(14) Liu, S.; Zhu, J.; Mastai, Y.; Felner, I.; Gedanken, A. *Chem. Mater.* **2000**, *12*, 2205.
(15) Pietrogiacomi, D.; Tuti, S.; Campa, M. C.; Indovina, V. *Appl. Catal. B−Environ.* **2000**, *28* (*1*), 43.
(16) Ileana, D.; Carrascullb, L. A.; Ponzib, M.; Ponzi, E. N. *Catal. Lett.* **2003**, *89*, 3.

10.1021/cm049830s CCC: $27.50
Published on Web 04/01/2004

in the presence of excess O_2. Orlik et al. have reported the role of the bifunctionality of $Co-ZrO_2$-based oxide systems in NO reduction with lower hydrocarbons.[17] Grams et al. performed temperature-programmed studies on carbon deposits[18] formed on ZrO_2-supported cobalt catalysts. The effect of the size distribution[19] of cobalt particles in Co/ZrO_2 system catalyst for the Fischer−Tropsch synthesis is reported by Chernavskii et al. Stefanov et al. also reported on the characterization[20] of $Co-ZrO_2$ de-NOX thin film catalysts prepared by magnetron sputtering. The ac electrical response[21] is studied in $Co-ZrO_2$ granular thin films composed of well-defined nanometric Co particles embedded in an insulating ZrO_2 matrix. Co−Zr−O nanogranular thin films[22] with improved high-frequency, soft magnetic properties is also reported by Ohnuma et al. The effect of microstructure, grain size, and rare earth doping on the electrorheological performance of nanosized ZrO_2 particles was studied and it was concluded that tetragonal ZrO_2 possess higher electrorheological activity[23] than monoclinic ZrO_2. However, complicated apparatus, complex process control, and special conditions are required for these approaches.

The major objective of the present report is to discuss a new process that uses a single-precursor, one-step reaction under autogenic pressure at elevated temperature (RAPET) without external catalyst and without a stabilizing agent to fabricate metastable fcc Co and tetragonal ZrO_2 phases. The reaction, which is the subject of this paper, is the dissociation of $CoZr_2(acac)_2(O^iPr)_8$ at 700 °C. Two main products result from the thermal dissociation of the precursor. They are two spherical particles: the first is a core−shell structure with Co as the core and carbon as the shell, and the second product is a core−shell structure where metastable tetragonal ZrO_2 particles are surrounded by a carbon shell. The products of the reaction were characterized by powder XRD, elemental (C, H, N, S) analysis, EDS, SAEDS, TEM, HR-TEM, Raman spectroscopy, and magnetic measurements.

Experimental Section

1. Synthesis and Gas-Phase Behavior of Precursor Compounds. $Zr_2(O^nPr)_2(O^iPr)_6(^iPrOH)_2$ (**1**) was obtained in practically quantitative yield by recrystallization of "$Zr(O^nPr)_4$" (purchased from Aldrich) in 2-propanol according to ref 24. $CoZr_2(acac)_2(O^iPr)_8$ (**2**) was obtained with quantitative yields by refluxing stoichiometric amounts of $Co(acac)_2$ (purchased from Aldrich and purified by sublimation in vacuo at 142−145 °C) and $Zr_2(O^iPr)_8(^iPrOH)_2$ (purchased from Aldrich and used without further purification) in toluene with subsequent evaporation to dryness and recrystallization from *n*-hexane, according to ref 24.

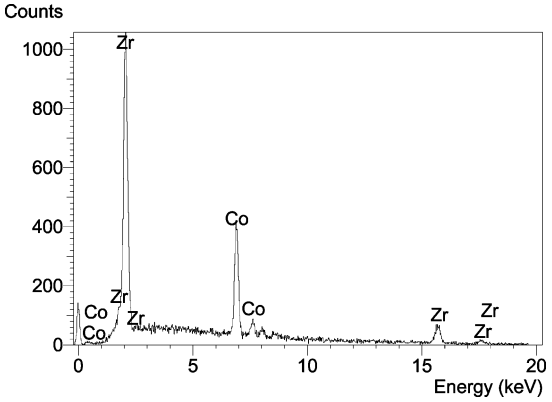

Figure 1. EDX of the CCZN product.

Both **1** and **2** are highly volatile and can be sublimed under mild conditions (140−150 °C/0.01 mmHg), **1** with decomposition, while **2** without noticeable decomposition under these conditions. The mass spectrum of **2** (JEOL JMS−SX/SX-102A mass spectrometer applying electron beam ionization at $U =$ 70 eV with direct probe introduction) contains, along with the fragmentation series of the molecular ion (with such ions as $[M - acac - CH_3]^+$ at $m/z = 795$, $[M - 2OR]^+$ at $m/z = 791$, and $[M - acac - OR]^+$ at $m/z = 751$), the fragmentation series corresponding to dissociation of the initial molecule into homometallic components such as $Co(acac)_2$ ($m/z = 257$), $Zr(acac)_2(O^iPr)_2$ [starting with the $Zr(acac)_2(O^iPr)^+$ ion at $m/z =$ 347], and $Zr(O^iPr)_4$ [m/z= 326 with $[Zr(O^iPr)_4 - CH_3]^+$ at m/z = 311 (100%) as the most intensive ion].

2. Fabrication of Co and ZrO_2 Nanoparticles Separately Coated with Carbon via RAPET Reactions. The fabrication of the metastable Co/C and metastable ZrO_2/C nanoparticles is carried out by introducing the $CoZr_2(acac)_2(O^iPr)_8$, i.e., $CoZr_2(CH_3COCHCOCH_3)_2(OC_3H_7\text{-}i)_8$, precursor in a 2 mL closed vessel cell. The cell is assembled from stainless steel Swagelok parts. A $^1/_2$ in. union part is plugged from both sides by standard caps. For these syntheses, 0.5 g of the above precursor is introduced in the cell at room temperature under nitrogen (nitrogen-filled glovebox). The filled cell is closed tightly by the other cap and then placed inside an iron pipe in the middle of a furnace. The temperature is raised at a heating rate of 10 °C/min. The closed vessel cell is heated at 700 °C for 3 h. The reaction took place under the autogenic pressure of the precursor. The cell is gradually cooled (∼5 h) to room temperature and opened, and a black powder is obtained. The total yield of product material is about 55% of the total weight of $CoZr_2(acac)_2(O^iPr)_8$ introduced in the cell. (The yield is the final weight of the product relative to the weight of the starting material.) The obtained two products are termed as carbon-coated cobalt (CCC) and carbon-coated zirconia (CCZ). Since these two different products are obtained in the same reaction from a single precursor, the composite is termed a carbon-coated cobalt/zirconia nanocomposite (CCZN) sample. We termed this new method for the synthesis of various nanomaterials as "reaction under autogenic pressure at elevated temperatures" (RAPET). Using this method recently we have prepared uniform, monodispersed carbon spherules[25] and nanosized Si-coated carbon spheres.[26] The present RAPET method for the synthesis of nanomaterials requires simple equipment, comparatively low temperature, and a short reaction time, and it produces core−shell morphology as a clean product.

(17) Orlik, S. N.; Struzhko, V. L.; Mironyuk, T. V.; Tel'biz, G. M. *Kinetics and Catalysis* **2003**, *44* (*5*), 682.
(18) Grams, J.; Goralski, J.; Paryjczak, T. *Przem. Chem.* **2003**, *82* (*3*), 161.
(19) Chernavskii, P. A.; Pankina, G. V.; Lermontov, A. S.; Lunin, V. V. *Kinet. Catal.* **2003**, *44* (*5*), 657.
(20) Stefanov, P.; Atanasova, G.; Marinova, T.; Gomez-García, J.; Sanz, J.; Caballero, M. A.; Morales, J. J.; Cordon, A. M.; Gonzalez-Elipe, A. R. *Catalysis Lett.* **2003**, *90*, 3.
(21) Hattink, B. J.; Labarta, A.; del Muro, M. G.; Batlle, X.; Sanchez, F.; Varela, M. *Phys. Rev. B* **2003**, *67* (*3*), 033402.
(22) Ohnuma, S.; Lee, H. J.; Kobayashi, N.; Fujimori, H.; Masumoto, T. *IEEE Trans. Magnetics* **2001**, *37* (*4*), 2251.
(23) Ma, S. Z.; Liao, F. H.; Li, S. X.; Xu, M. Y.; Li, J. R.; Zhang, S. H.; Chen, S. M.; Huang, R. L.; Gao, M. S. *J. Mater. Chem.* **2003**, *13* (*12*), 3096.
(24) Kessler, V. G.; Seisenbaeva, G. A. Influence of Heteroligands on the Composition, Structure and Properties of Homo- and Heterometallic Zirconium Alkoxides. Contrib. Materials Discussion 7, to be submitted to *J. Mater. Chem.*
(25) Pol, V. G.; Motiei, M.; Gedanken, A.; Calderon-Moreno, J.; Yoshimura, M. *Carbon* **2004**, *42*, 111.
(26) Pol, V. G.; Pol, S. V.; Gofer, Y.; Calderon-Moreno, J.; Gedanken, A. *J. Mater. Chem.* **2004**, *14*, 966. DOI: 10.1039/<b300001a>.

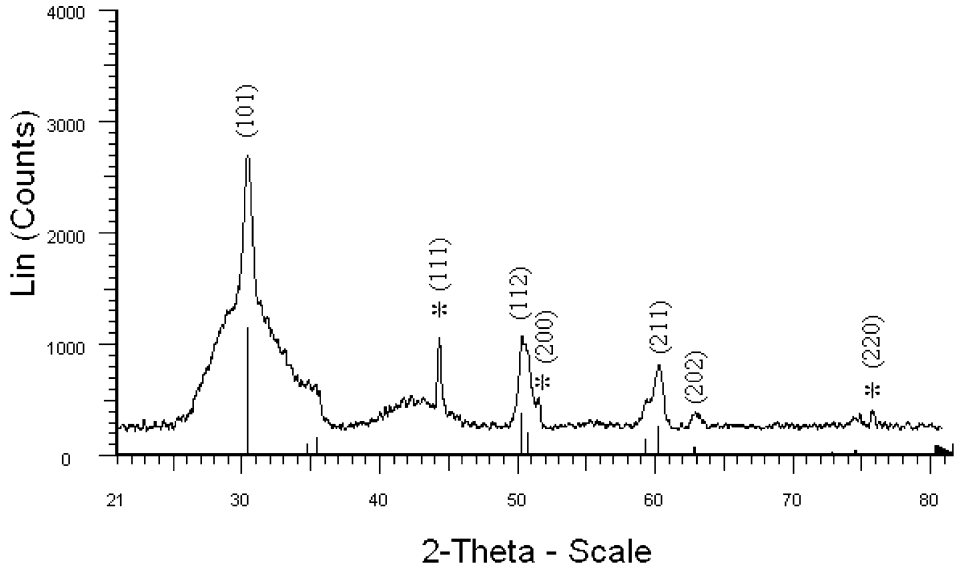

Figure 2. Powder XRD pattern of a CCZN sample.

3. Characterization. The CCZN composite was characterized by various structural, morphological, and magnetic techniques. XRD patterns were collected by using a Bruker AXS D* Advance powder X-ray diffractometer (Cu Kα radiation, wavelength 1.5406 Å). The morphologies and nanostructure of the as-synthesized products were further characterized with a JEM-1200EX TEM and a JEOL-2010 HRTEM using an accelerating voltage of 80 and 200 kV, respectively. SAEDS (selected area energy dispersive X-ray analysis) of one individual particle was conducted using a JEOL-2010 HRTEM model and EDX was done using an X-ray microanalyzer (Oxford Scientific), both attached to a JSM-840 scanning electron microscope (SEM). Samples for TEM and HRTEM were prepared by ultrasonically dispersing the products into absolute ethanol, placing a drop of this suspension onto a copper grid coated with an amorphous carbon film, and then drying in air. A Scion image software program was used to measure the mean particle size of the core of ZrO_2 or Co nanoparticles. The elemental analysis of the samples was carried out by an Eager 200 C, H, N, S analyzer. An Olympus BX41 (Jobin Yvon Horiba) Raman spectrometer was employed, using the 514.5 nm line of an Ar laser as the excitation source to analyze the nature of the carbon present in the CCZN material. Magnetic measurements of the CCZN material were performed on a vibrating sample magnetometer (VSM-Oxford-3001).

Results and Discussion

1. Elemental (C, H, N, S) Analysis, Energy-Dispersive X-ray Analysis (EDX), and X-ray Diffraction (XRD) Measurements. The content of carbon and hydrogen in the product/carbonaceous material was determined by an elemental analysis measurement. We have calculated the element (wt) percent in the $CoZr_2(acac)_2(O^iPr)_8$ and compared it with elemental analysis data of the CCZN product. The calculated percent of carbon in $CoZr_2(acac)_2(O^iPr)_8$ is 44.76% (in 0.5 g of precursor) while the percentage of hydrogen is 7.68%. The respective measured element percentage of carbon in the CCZN product is 9.73% (in 0.275 g of product), while the percentage of hydrogen is 0.08%. It is observed that the products show a drastic loss of carbon and hydrogen. It is suggested that the weight loss of carbon and hydrogen is due to the formation of hydrocarbons, which exit the cell as the result of the release of pressure while opening the Swagelok cell.

The presence of zirconium, cobalt, carbon, and oxygen in the CCZN material was examined by EDX measurement (Figure 1). The EDX spectrum was also used to obtain a quantitative estimate of the Zr and Co. For the light elements such as oxygen and carbon, only a rough estimate could be obtained. In the CCZN product the percentage (wt) of Zr and Co are 73% and 27%, respectively.

The XRD pattern of the CCZN sample is presented in Figure 2. The major peaks and their intensities at 2θ values of 30.24°, 50.25°, 60.24°, and 62.89° correspond to the reflection lines of the metastable tetragonal phase of zirconia. These values are in good agreement with the diffraction peaks, peak intensity, and cell parameters of crystalline ZrO_2 (PDF No. 79-1770). The peak widths, for the metastable tetragonal phase of zirconia, at half-peak height, are wide, indicating the small crystallite sizes (∼11−16 nm). The diffraction lines indicated by stars are assigned to the crystalline face-centered cubic phase of cobalt (PDF No. 15-806). It is well-known that the transformation from the fcc to the stable hexagonal phase usually occurs[27] at 417 °C, while in the current reaction even at 700 °C the metastable phase is retained. This is because the change from the fcc to the hexagonal phase would require space, and it is hindered by the carbon coating. The same phenomenon was reported for Co encapsulated in carbon nanotubes.[14] No characteristic peaks of carbon were observed in the CCZN sample, and this might be due to its amorphous nature. Further evidence for its amorphous nature is given by the Raman spectroscopy measurements (Figure 5). The high stability of metastable fcc cobalt and tetragonal zirconia is related to the in situ formed protective carbon shell. It is demonstrated for example when the samples are aged in air atmosphere at room temperature. XRD measurements after a few months at ambient conditions did not detect any changes in the diffraction peaks.

2. Electron Microscopy Studies (LR-TEM, HR-TEM, and SAEDS). The morphology and structure of

(27) Dille, J.; Charlier, J.; Winand, R. *J. Mater. Sci.* **1998**, *33* (*11*), 2771.

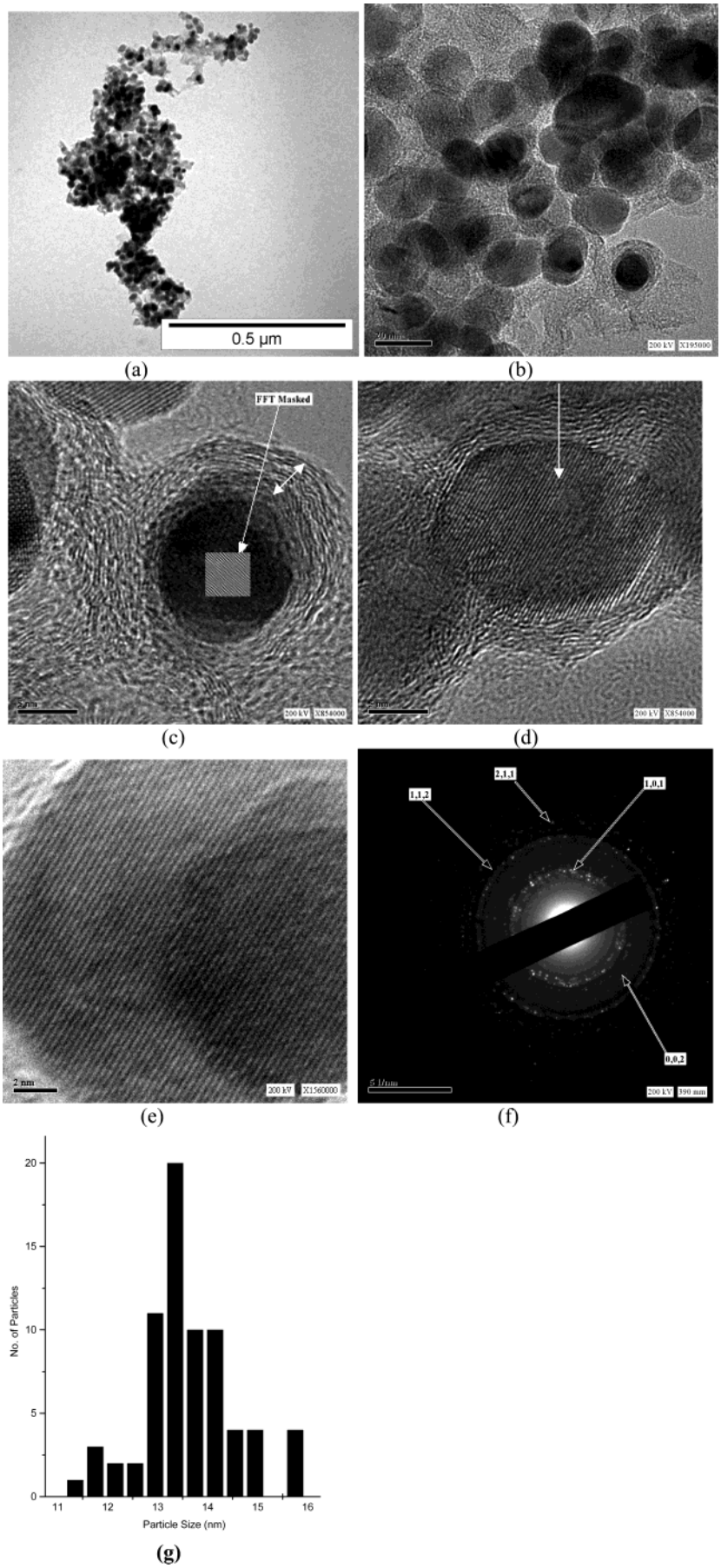

Figure 3. Images from the (a) LR-TEM of a CCZN sample, (b) HR-TEM of a CCZN sample (bar indicates 20 nm), (c) HR-TEM of a CCC particle and its masked fast Fourier transform (FFT) image (bar indicates 5 nm), (d) HR-TEM of a CCZ particle (bar indicates 5 nm), (e) core of a CCZ particle shown at high resolution, (f) electron diffraction of part e, and (g) particle-size histogram obtained from the TEM picture (part a), using Scion image software program.

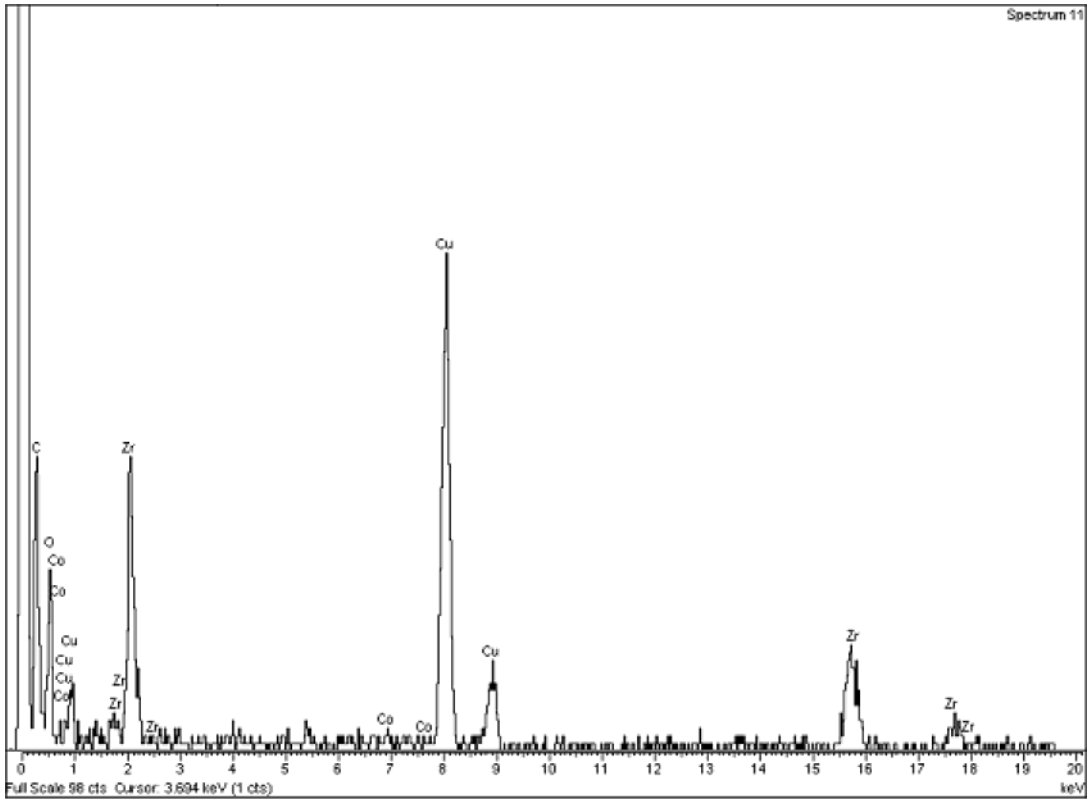

Figure 4. SAEDS of a carbon-coated zirconia particle.

a CCZN sample were studied by LR-TEM and HR-TEM measurements. Figure 3a depicts spherical particles coated with a nanolayer of a material having a different contrast. The analysis of the HR-TEM results shows that the product is composed of two different particles, namely carbon-coated cobalt (CCC) and carbon-coated zirconia (CCZ). In both the cases Co and zirconia nanoparticles form the cores and are homogeneously embedded in a carbon shell, having a core−shell structure (Figure 3b). The diameter of these cores is ∼13 nm and the outer carbon shell is ∼4 nm (Figure 3, parts c, marked by double sided arrow, and d). The stabilization of Co or ZrO_2 cores is due to the carbon shell, which is not allowing a change of the metastable phases.

A similar RAPET reaction was carried out at 700 °C, by introducing $Zr_2(O^nPr)_2(O^iPr)_6(^iPrOH)_2$ precursor in a 2 mL closed vessel cell. It leads to the formation of separate zirconia and carbon particles without core−shell structures. The formed nanosized zirconia shows mostly monoclinic and very small tetragonal phase. This proves that only after a uniform layer of carbon is formed on the surface of zirconia is stabilization of the metastable phase realized. The separate growth of zirconia and carbon in this case is typical of decomposition of metal alkoxides not substituted by acetylacetonate ligands, which is characterized by lower volatility and hindered nucleation that leads to bigger particles and nonuniform growth through the gas-phase transport.[28] Another explanation for the absence of a carbon shell in the decomposition of $Zr_2(O^nPr)_2(O^iPr)_6(^iPrOH)_2$ is the lack of Co. We believe that although the CCZ (ZrO_2(tetragonal)/C) is composed mostly of zirconia, a small amount of cobalt atoms (observed in the SAEDX) exist in the zirconia core. Cobalt is well-known as a catalyst for the growth of carbon around it.

The assignment of "core" to Co and ZrO_2 and "shell" to carbon is based on the SAEDS and HR-TEM techniques presented below. We assume that the dissociation of $CoZr_2(acac)_2(O^iPr)_8$ at such high temperature as 700 °C leads primarily to formation of highly volatile homometallic acetylacetonato-alkoxides of zirconium and of cobalt, in analogy to the dissociation caused by the electron beam impact in the mass spectrometric experiment. Further destruction in the gas phase results in uniform multicenter nucleation and rapid simultaneous growth of highly crystalline, almost spherical particles of the high-energy phases of ZrO_2 and of metallic Co (due to reduction by the organic residues). Lowering of the gas phase concentration of metal−organic precursors results subsequently in catalytic thermal decomposition of the purely organic components on the surface of nanoparticles, resulting in the core−shell structure. The reaction mechanism for the particle growth involves in this case, supposedly, the reactions of ether and β-elimination, which are typical for transition-metal metal−organic decomposition.[28] In the case of RAPET of the tetraethyl orthosilicate (TEOS), we could account for the solidification of the carbon[26] as the spherical core, both thermodynamically and kinetically, as the thermolysis in that latter case was proceeding most likely via radical mechanisms more typical for the organosilicon compounds. The HR-TEM of a CCC particle depicted in Figure 3c provides further evidence for the identification of the Co core. It illustrates the perfect arrangements of the atomic layers and the lack of defects. The measured distance between these (111) lattice planes is 0.21 nm, which is very close to the

(28) Scheglov, P.; Seisenbaeva, G. A.; Gohil, S.; Drobot, D. V.; Kessler, V. G. *Chem. Mater.* **2002**, *14*, 2378 (and references therein).

distance between the planes reported in the literature (0.204 nm) for the face-centered cubic lattice of the Co (PDF: 15−806).

The HR-TEM of a CCZ particle depicted in Figure 3d provides evidence for the existence of the tetragonal ZrO_2 core (marked by an arrow). It illustrates the perfect arrangements of the atomic layers and the lack of defects. The measured distance between these (101) lattice planes is 0.294 nm (Figure 3e), which is very close to the distance between the planes reported in the literature (0.295 nm) for the tetragonal phase of the ZrO_2 (PDF: 79−1770). The disordered and ordered carbon layers (Figure 3c,d) were detected in the HR-TEM image. Carbon has a tendency to form a very uniform shell of ∼4 nm on the surface of Co or ZrO_2 nanoparticles. Interlayer spacing in the coated carbon is ∼0.35 nm, very close to the distance between graphitic layers. Figure 3f presents the selected area electron diffraction for the CCZ particle depicted in Figure 3e. The obtained electron diffraction data matches with various planes (shown by an arrow) of tetragonal zirconia. More evidence for the amorphous nature of carbon is the lack of electron diffraction or fast Fourier transform (FFT) images. On the contrary, Co and ZrO_2 produce electron diffraction or FFT. A statistical analysis of the histogram obtained from the TEM picture (Figure 3a) shows that the mean size of the core of ZrO_2 or Co nanoparticles is 13.3 ± 0.1 nm. The histogram reveals (Figure 3e) a narrow size distribution of particles, which according to the TEM are monodispersed.

To further substantiate our identification of the core−shell structure, SAEDS measurements were performed. A 25 nm electron beam was focused on the center of a CCZ particle and confirmed zirconia as a core. The typical SAEDS presented in Figure 4 shows the presence of a small amount of Co and large amounts of Zr, O, C, and Cu. The carbon and Cu peaks are always originating from the TEM grid. Since the particle size of zirconia is ∼12 nm, the electron beam overlaps an adjacent Co particle. This is the reason that Co is also detected.

3. Raman Spectroscopy and Magnetic Measurements. Raman spectroscopy measurements were performed to understand the nature of the carbon coating in the CCZN sample. The micro-Raman spectrum of the CCZN sample is shown in Figure 5. The two characteristic bands of carbon were detected at 1341 cm^{-1} (D-band) and 1596 cm^{-1} (G-band).[29] The intensity of the G-band, associated with graphitic carbon, is smaller than the intensity of the D-band. The intensity ratio of the D- and G-bands is $I_D/I_G = 1.2$ for the CCZN sample. It is suggested that the existence of the nongraphitic layers is due to the execution of the RAPET reaction at 700 °C, which is not high enough to permit improvement of the local order of the deposited carbon.

The magnetic properties were investigated by magnetic susceptibility measurements as outlined in the Experimental Section. The magnetization vs magnetic field curve for the CCZN sample shows a ferromagnetic[14] behavior (Figure 6). The saturation magnetizations M_s and coercivity are 18 emu $g^{-1}$and ∼70 Oe, respectively, for the CCZN sample. Taking into account the weight of cobalt present in the entire material (from EDAX), the saturation magnetization of CCZN sample works out to more than 60 emu g^{-1}.

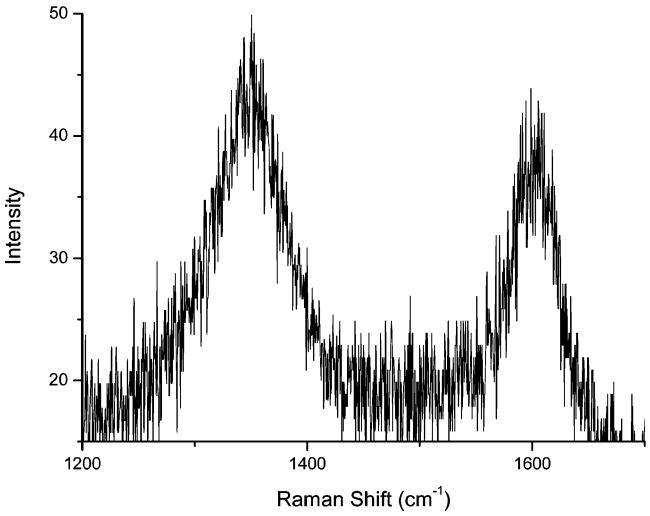

Figure 5. Raman spectrum of a CCZN sample.

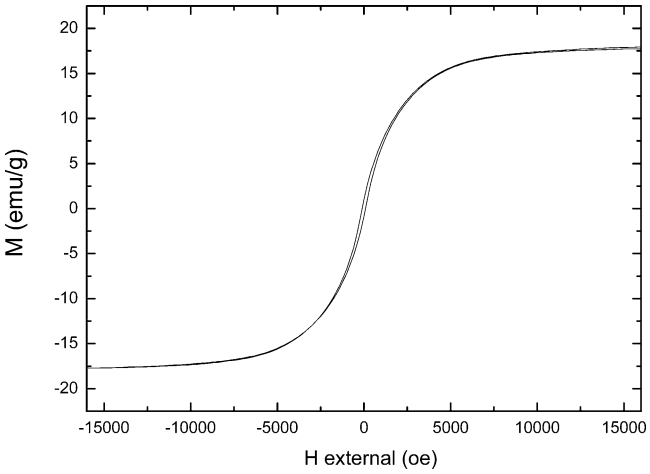

Figure 6. The magnetization vs magnetic field curve for a CCZN sample.

Conclusions

In conclusion, the novel one-step RAPET of $CoZr_2(acac)_2(O^iPr)_8$ at 700 °C, in the absence of catalyst, led to the formation of core−shell composites. Metastable phases of separate Co and ZrO_2 particles that are coated with carbon are identified. For the first time, using RAPET technique and without doping any trivalent impurities, spherical ZrO_2 particles exhibiting metastable tetragonal crystal structure at room temperature are obtained. According to our interpretation, based on high-resolution transmission electron microscopy and selected area energy-dispersive X-ray analysis, the ∼4 nm carbon shell on the surface of ZrO_2 and Co nanocrystallites is responsible for stabilizing the high-temperature metastable tetragonal and fcc phase, respectively, at room temperature.

CM049830S

(29) Dresselhaus, M. S.; Dresselhaus, G.; Pimenta M. A.; Eklund, P. C. In *Analytical Application of Raman Spectroscopy;* Pelletier, M. J., Ed.; Blackwell Science: Oxford, 1999; Chapter 9.